Superlocalization of the Electronic Wave Functions in Conductive Polymer Blends at Concentrations near the Percolation Threshold

M. Reghu, C. O. Yoon, C. Y. Yang, D. Moses, and A. J. Heeger*,†

Institute for Polymers and Organic Solids, University of California at Santa Barbara, Santa Barbara, California 93106

Y. Cao

UNIAX Corporation, 5375 Overpass Road, Santa Barbara, California 93111

Received May 10, 1993; Revised Manuscript Received July 19, 1993•

ABSTRACT: The ability to solution-process polyaniline (PANI) in the protonated conducting form through the use of surfactant counterions has enabled the fabrication of conductive polymer blends with a percolation threshold at a volume fraction near 1%. Electron micrographs of blends of PANI complexed with camphorsulfonic acid (CSA) in poly(methyl methacrylate) show a tenuous interconnected network; for concentrations of PANI–CSA near the percolation threshold, the network is self-similar. Digital analysis of the micrographs shows that in thin two-dimensional "slices" the PANI–CSA networks are fractal, with the area (S) of the conducting network varying as $S \propto r^D$, where $D < 2$ for concentrations below 4%. Near the threshold, we find $D \approx 1.5$, implying a fractal dimensionality in three dimensions of ca. 2.5. The electrical conductivity of these blends follows the Mott–Deutscher model for variable-range hopping on a fractal network, $\sigma(T) \sim \exp[-(T_0/T)^\gamma]$. We find that γ increases from $\gamma = {}^1/_4$ in pure PANI–CSA (indicting variable-range hopping among exponentially localized states) to $\gamma \approx {}^2/_3$ as the PANI–CSA concentration is reduced to the percolation threshold, indicating variable-range hopping among superlocalized states on the fractal structure in the limit where the Coulomb interaction between the electron and the hole dominates the intersite hopping.

Introduction

Conducting polymer blends are a new class of materials in which the threshold for the onset of electrical conductivity (σ) can be reduced to volume fractions well below that required for classical percolation (16% by volume for globular conducting objects dispersed in an insulating matrix in three dimensions).[1–5] Due to the low percolation threshold and the continuous increase of $\sigma(f)$ for volume fractions (f) above the threshold, conducting polyblends can be reproducibly fabricated with controlled levels of electrical conductivity while retaining the desired mechanical properties of the matrix polymer.[2]

Within the class of conducting polymers, polyaniline (PANI) is especially attractive: PANI is unique in that it is soluble, and therefore processible, in the conducting form;[6] and it is both thermally and environmentally stable. Protonation of the emeraldine base form of PANI with functionalized sulfonic acids (functionalized such that after protonation the counterion in the conducting emeraldine salt is a surfactant) renders PANI soluble *in the conducting form* in common organic solvents.[6] Conducting polyblends can be made by codissolving the conducting PANI complex and a suitable matrix polymer in a common solvent and processing the conducting blend directly from solution.[6–8] Homogeneous high-quality films of these conducting blends can be easily prepared for analysis and for electrical measurements by casting from solution.[7]

We present the results of a study of conducting blends of PANI complexed with camphorsulfonic acid (CSA) in poly(methyl methacrylate) (PMMA) in the concentration range near the percolation threshold. Electron micrographs of the PANI–CSA/PMMA blends in this range of concentrations show a tenous interconnected network.[8] For concentrations of PANI–CSA near the percolation threshold, the network is self-similar; digital analysis of the micrographs shows that the PANI–CSA networks are fractal, with the area (S) of the conducting network varying as $S \propto r^D$, where $D < 2$ for concentrations below 4%. Near the percolation threshold at $f_c \approx 0.01$, we find $D \approx 1.5$, implying a fractal dimensionality of the three-dimensional blends of ca. 2.5. The electrical conductivity of these blends follows the temperature dependence given by the Mott–Deutscher model for variable-range hopping on a fractal network, $\sigma(T) \propto \exp[-(T_0/T)^\gamma]$. We find that γ increases from $\gamma = {}^1/_4$ in the bulk material (indicating variable-range hopping among exponentially localized states) to $\gamma \approx {}^2/_3$ as the PANI–CSA concentration is reduced to the percolation threshold, indicating superlocalization of the electronic wave functions on the fractal structure in the limit where the Coulomb interaction between the electron and the hole dominates the intersite hopping.

Sample Preparation and Electron Microscopy

PANI–CSA solutions are prepared dissolving the emeraldine base form of PANI and CSA at 0.5 molar ratio of CSA to phenyl-N repeat unit in *m*-cresol.[6] This solution is then mixed in appropriate ratio with a solution of PMMA in *m*-cresol. Films of thickness 20–40 μm were obtained by casting the blend solution onto a glass plate. After drying at 50 °C in air for 24 h, the polyblend film was peeled off the glass substrate to form a free-standing sample for electrical measurements. The temperature dependence of the electrical conductivity of the PANI–CSA/PMMA blends was measured by the four-terminal dc method over the temperature range from 300 to 10 K.

Ultrathin films for transmission electron microscopy (TEM) studies were prepared as described previously.[8] Transmission electron micrographs of films in the concentration range 0.5–4.8% (w/w) show an interpenetrating network of PANI–CSA in the PMMA matrix.[8] The density of the interconnected network is dependent on the concentration of PANI–CSA in the blend; the organization of conducting polymer as a network of interconnected pathways is observed at all concentrations, but the density of connected paths varies with the concentration of PANI–CSA, as shown in Figure 1. Examination of the TEM picture implies that the onset of macroscopically connected pathways

* To whom correspondence should be addressed.
† Department of Physics and Materials Department, UCSB.
• Abstract published in *Advance ACS Abstracts*, October 1, 1993.

0024-9297/93/2226-7245$04.00/0

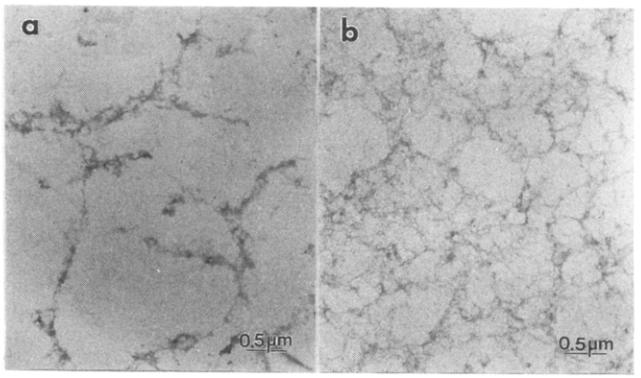

Figure 1. Transmission electron micrographs of extracted PANI–CSA/PMMA polyblend films containing (a) 0.96% (w/w) and (b) 1.96% (w/w) PANI–CSA.

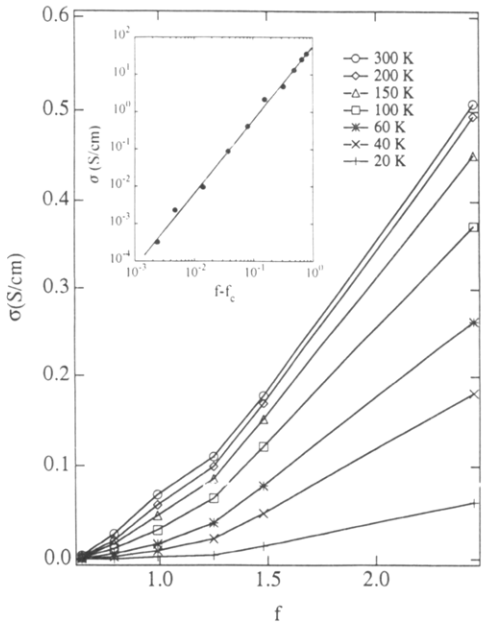

Figure 2. Conductivity (σ) vs volume fraction (f) of PANI–CSA at different temperatures. The inset shows log σ vs log $(f - f_c)$ above the percolation threshold ($f_c \approx 0.01$) for $T = 10$ K; the solid line through the points corresponds to a slope of 1.97 ± 0.02, the best fit from a linear regression analysis with various trial values for f_c.

(the percolation threshold) occurs at ca. 1% wt/wt of PANI/CSA in PMMA.

Fractal Structure near the Percolation Threshold

The interpenetrating network morphology of PANI–CSA in PMMA self-assembles during liquid–liquid phase separation. The tenuous "stringy" network of conducting pathways results from a compromise: the surfactant counterions want to be at the interface between the polar PANI (a salt) and the weakly polar PMMA, whereas the PANI and PMMA tend to phase separate (since there is no entropy of mixing for macromolecules). The result is a phase-separated structure with high surface area, i.e., the open fibrillar structure shown in Figure 1. The low percolation threshold results directly from this self-assembled fibrillar network morphology.

Figure 1 and the $\sigma(f)$ vs f data indicate that the percolation threshold occurs near $f \approx 0.01$. The percolation threshold can be identified with greater precision by measuring the temperature dependence of the conductivity of blends containing varying concentrations of PANI–CSA near the threshold. Figure 2 shows the conductivity of samples having concentrations $f = 0.005$, 0.0065, 0.008, 0.01, 0.0125, 0.015, and 0.025 PANI–CSA in PMMA; the data are presented as $\sigma(f)$ vs f for a series of temperatures between 300 and 20 K. Since there is a well-defined increase in the slope of σ(f) at $f \approx 0.01$–0.0125 PANI–CSA at all temperatures, we identify $f_c \approx 0.01$–0.0125 as the percolation threshold.

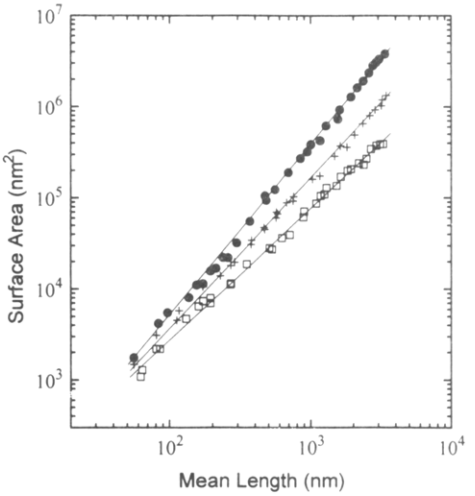

Figure 3. log–log plot of surface area vs the geometrical mean length for $f = 0.037$ (solid dots), 0.0196 (pluses), and 0.0096 (solid squares).

To identify the percolation threshold more precisely, we have fit the data to the scaling law of percolation theory,[9]

$$\sigma(f) = C|f - f_c|^t \quad (1)$$

where f_c is the critical percolation threshold, C is a constant, and t is the critical exponent. From such fits, one can determine both the critical volume fraction (f_c) and the exponent (t). The best fit of the low-temperature data (10 K) to the power law dependence of eq 1, as determined from a linear regression analysis with various trial values of f_c, is obtained with $f_c = 0.011$ (± 0.002); the data are plotted as log σ vs log$(f - f_c)$ in the inset of Figure 2. The slope of the solid line on the log–log plot yields the critical exponent, $t = 1.97 \pm 0.02$. This values is in agreement with the predicted universal value ($t = 2$)[9] and in agreement with the value reported for carbon black/polymer composites[10] and other related systems near the percolation threshold.[9]

As noted earlier,[8] the structure of the interconnected fibrillar network appears to be self-similar, especially at concentrations near $f \approx 0.01$. The appearance of self-similarity is consistent with the well-known result that all systems are fractal near the percolation threshold on length scales below the correlation length of the percolating cluster.[9]

The fractal structure of the interconnected network shown in Figure 1 has been confirmed through numerical analysis of the TEM micrographs. The TEM photographs of the blends with various concentrations of PANI–CSA were digitized to binary images using an image scanner. The digitized images were then checked to verify that the digitized networks closely coincided with those on the original micrographs. The projected surface area (S) of the PANI–CSA aggregates was counted inside a series of rectangles with dimensions chosen on successively larger length scales.[11] In general, one expects a power law relationship between the mass M (or the area, S) and the size of fractal aggregates:[9]

$$M(r) \propto r^D \quad (2)$$

where D is the fractal dimension. As shown in Figure 3,

the log–log plots of S vs the geometric mean of the length times the width of the enclosed rectangle yield straight lines with slope dependent on the volume fraction of PANI–CSA in the blend; $D = 1.99, 1.75, 1.53$ for $f = 0.037$, 0.0196, and 0.0096, respectively.

For $f \approx 0.037$ (and above), $D = 2$, indicating that the network is sufficiently dense and uniform that the blend can be considered an effective medium; the fractal dimensionality is the same as the spatial dimensionality. As f is decreased toward the percolation threshold, D becomes less than the spatial dimensionality, indicating a self-similar structure with holes on every length scale. At $f \approx f_c$, we find $D \approx 1.5$.

The fractal dimensionality of the percolating cluster is not universal, D_c will depend on the nature of the percolating objects (for example, globules vs rods). In the site percolation model, the values of D in two (three) dimensions are 1.9 (2.5) for $f = f_c$ and 1.6 (2) for $f < f_c$.[9] Based on the high aspect ratio of the components which form the open network morphology of the PANI–CSA/PMMA blends, we expect that the observed $D_c \approx {}^3/_2$ will be characteristic of percolating rods. This implies that for rod-shaped percolating objects the connectivity increases more rapidly with f,[1b] while the growth of the cluster size is slower with respect to the length scale of the system.

By analyzing the TEM images of ultrathin films, we have determined the fractal dimension of a two-dimensional "slice" of the three-dimensional object. Since the film thickness of ca. 100 Å is much less than the typical dimensions of the clusters which form the network, shadowing is not important. Thus, the two-dimensional analysis should be accurate. Moreover, the determination of the fractal dimension of the three-dimensional network (D_3) from the two-dimensional slice (D_2) is straightforward; since the slice is thin with negligible shadowing, $D_3 \approx D_2 + 1$. Therefore, near the percolation threshold, $D_3 \approx 2.5$.

Variable-Range Hopping among Superlocalized States

Levy and Souillard[12] have shown that the solutions to the Schrödinger equation on a fractal structure are "superlocalized". For a conductor, the wave functions for states near the Fermi level decay as $\psi(r) \propto \exp[-(r/L_c)^\xi]$, where L_c is the localization length and $\xi > 1$, rather than exponentially ($\xi = 1$) as would be the case for conventional disorder-induced localization (Anderson localization).[13] Deutscher, Levy, and Souillard[14] predicted that the temperature dependence of the electrical conductivity which results from variable-range hopping between such superlocalized states would be of the form

$$\sigma(T) \propto \exp[-(T_0/T)^\gamma] \qquad (3)$$

where T_0 is a characteristic temperature and $\gamma > {}^1/_4$ ($\gamma = {}^1/_4$ corresponds to variable-range hopping among exponentially localized states).[13] For the case where Coulomb effects are relatively unimportant, $\gamma = \xi/(D + \xi)$,[14] whereas when the Coulomb interactions dominates the hopping transport, $\gamma = \xi/(\xi + 1)$.[15]

This unusual temperature dependence (eq 3) was reported by van der Putten et al.[15] for carbon black/polymer composites at volume fractions of the carbon black filler near the percolation threshold. For these filled polymers, the best fit to $\sigma(T)$ is in agreement with eq 3 with $\gamma \approx {}^2/_3$ ($\gamma = 0.66 \pm 0.02$). This experimentally determined value is somewhat larger than that predicted by Deutscher, Levy, and Souillard;[14] with the assumptions that $\xi = d_w/2$, where d_w is the dimension of a random walk on a fractal ($d_w/2 = 1.90$ on the incipient percolating cluster in three dimensions) and that the Alexander–Orbach conjecture ($2D/d_w = {}^4/_3$) is valid,[16] Deutscher, Levy, and Souillard[14] predicted $\gamma = {}^3/_7$.

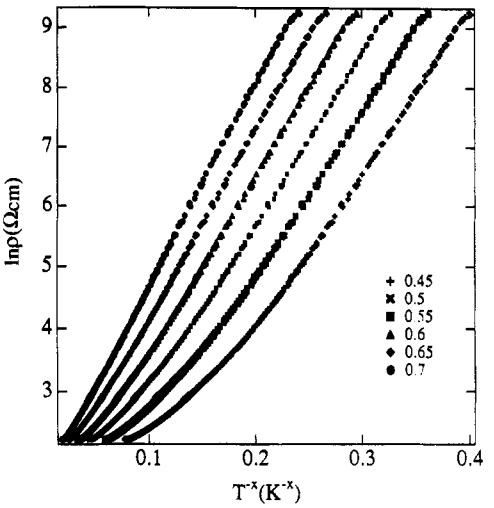

Figure 4. Natural logarithm of resistivity vs $T^{-\gamma}$, for $0.45 < \gamma < 0.7$, for $f = 0.0125$ PANI–CSA in PMMA.

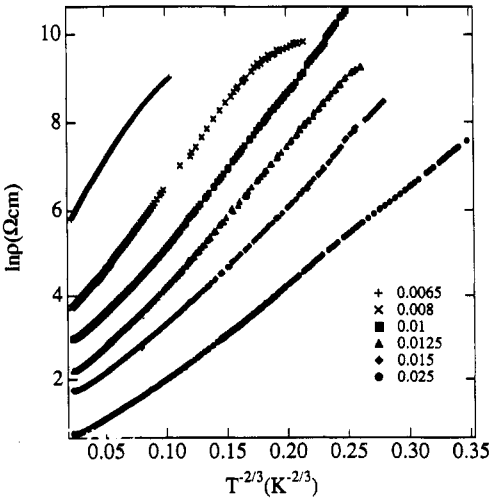

Figure 5. Natural logarithm of resistivity vs $T^{-2/3}$ for $f = 0.0065$, 0.008, 0.01, 0.0125, 0.015, and 0.025 PANI–CSA in PMMA.

Applying these concepts to the PANI–CSA/PMMA blends suggests that as the volume fraction of PANI–CSA is reduced, the conductivity will follow the generalized variable range hopping expression (eq 3), with γ increasing from ${}^1/_4$ in pure PANI–CSA (where the residual disorder induces localization with the Fermi level close to the mobility edge[7]) to a value characteristic of hopping among superlocalized states for f near f_c.

The temperature dependence of conductivity of the sample with $f \approx f_c$ ($f_c = 0.01$) is plotted vs $T^{-\gamma}$ for various values of γ in Figure 4. The best linear fit is obtained with $\gamma = 0.66 \pm 0.04$, in close agreement with the dependence found for carbon black filled polymer composites close to the percolation threshold,[15] even though the morphologies of the conducting materials in the insulating matrices are rather different in the two cases.

As shown in Figure 5, the temperature dependence of the conductivity of PANI–CSA/PMMA for all samples with f in the range of $0.0064 < f < 0.025$ follows eq 3 over a reasonable temperature range with $\gamma = 0.66 \pm 0.04$ (although the room temperature conductivities of these blends vary by 4 orders of magnitude). The conductivity ratios and the values for T_0 (see eq 3) for these samples are shown in Table I. The values of T_0 are only weakly dependent on the concentration of PANI–CSA (for $f \leq$

Table I. Parameters of the Temperature Dependence of Conductivity at Various Concentrations (f) of PANI–CSA (by Weight) in PMMA

f	σ(300 K)/σ(10 K)	T_0 (K)
0.025	52	107
0.015	120	156
0.0125	366	181
0.0100	472	216
0.0080		225
0.0065		216

0.01, T_0 is nearly concentration independent). This weak concentration dependence is in agreement with the predicted behavior for variable-range hopping among superlocalized states on a fractal network.[14]

Using the Deutscher–Levy–Souillard expression,[14] $1/\gamma = 1 + D_3/\xi$ (we emphasize that the transport data were obtained from three-dimensional samples), and the experimentally determined value for the fractal dimensionality, $D_3 \approx {}^5/_2$, we obtain $D_3/\xi \approx {}^1/_2$ and $\xi = 2D_3 \approx 5$, considerably greater than that predicted by Levy and Souillard.[12]

The theory of variable-range hopping among superlocalized states was generalized by van der Putten et al.[15] to include the Coulomb interaction between the electron and the hole, i.e., the analogue of the Efros–Shklovskii theory[19] for variable-range hopping among exponentially localized states. When the Coulomb interaction is important, van der Putten et al.[15] find that $\sigma(T)$ follows eq 3 with $\gamma = \xi/(1 + \xi)$. Using this expression for γ and the experimentally determined value, $\gamma = 0.66 \pm 0.04$, one finds $\xi \approx 1.98 \pm 0.35$, in agreement with the theoretical value[12] (see, however, the recent comments by Aharony et al.[17] and by Michels et al.[18]).

Importance of the Coulomb Interaction

The close agreement between γ obtained from the measurements of PANI–CSA/PMMA blends and γ obtained from the carbon black composites suggests that the same mechanism is dominant near the percolation threshold. On the other hand, measurements of $\sigma(T)$ for pure PANI–CSA ($f = 1$) indicate that the Coulomb interaction is effectively screened; there is no indication of the Efros–Shklovskii $\gamma = {}^1/_2$ dependence[19] even at temperatures as low as 1.2 K. Since the PANI–CSA remains phase separated at all volume fractions in the PANI–CSA/PMMA blends, one might argue that the Coulomb interaction would remain well screened and therefore would not play an important role in the hopping transport even in the regime of superlocalization.

As a possible resolution of this apparent contradiction, we suggest that with the onset of superlocalization in the blends the PANI–CSA system moves away from the boundary of the metal–insulator transition with a corresponding reduction in the metallic screening. The tendency for screening of the Coulomb interaction to become ineffective when the electronic states become superlocalized is probably quite general; near the threshold, the conductivity is low and the states are localized at distances much less than the localization length which would result from the microscopic disorder in the bulk material.

The proposed evolution of the relative importance of the Coulomb interactions to the transport is confirmed by the data. For concentrations below the percolation threshold, charge carriers feel the fractal nature of the system only at smaller length scales (smaller than the typical cluster size). Since the wave function falls off exponentially at larger length scales, conventional variable-range hopping among *exponentially* localized states will be restored at sufficiently low temperatures that intercluster hopping dominates the transport. As shown in Figure 5, the $\gamma = {}^2/_3$ fit deviates from linearity at low temperatures for samples containing less than 1% PANI–CSA. For blends containing 0.8% of PANI–CSA, the $\gamma = {}^2/_3$ fit deviates below 14 K such that at very low temperatures $\gamma \approx {}^1/_2$; for 0.65% PANI–CSA, the resistance is so high that the crossover cannot be observed in detail (although the deviation from the $\gamma = {}^2/_3$ dependence begins at even higher temperatures). Thus, the data indicate a crossover from $\gamma \approx {}^2/_3$ (characteristic of variable-range hopping among superlocalized states) to $\gamma \approx {}^1/_2$, characteristic of variable-range hopping among exponentially localized states in the Efros–Shklovskii limit.[19] Since the intercluster distances are relatively large, the prefactor is very small, but since the wave funtions fall off exponentially, the $\gamma = {}^1/_2$ dependence is restored.

Summary and Conclusion

In the concentration range near the percolation threshold, conducting blends of PANI complexed with camphorsulfonic acid in poly(methyl methacrylate) have a fractal microstructure which causes superlocalization of the electronic wave functions. Electron micrographs of the PANI–CSA/PMMA blends in this range of concentrations show a tenuous interconnected network which is self-similar; analysis of the micrographs yields a mass distribution varying as $M \propto r^D$ with $D \approx 1.5$, implying a fractal dimensionality of the three-dimensional blends of ca. 2.5. The electrical conductivity of these blends follows the temperature dependence of the Mott–Deutscher model for variable-range hopping on a fractal network, $\sigma(T) \propto \exp[-(T_0/T)^\gamma]$. We find that γ increases from $\gamma = {}^1/_4$ in the bulk material (indicating variable-range hopping among exponentially localized states) to $\gamma \approx {}^2/_3$ as the PANI–CSA concentration is reduced to the percolation threshold, indicating superlocalization of the electronic wave functions on the fractal structure.

The $\exp[-T_0/T)^\gamma]$ dependence with $\gamma \approx {}^2/_3$ is consistent with the theory of variable-range hopping among superlocalized states in the limit where the Coulomb interaction between the electron and the hole dominates.[15] Using $\gamma = \xi/(1 + \xi)$ as appropriate for strong Coulomb interactions and the experimental value for $\gamma = 0.66 \pm 0.04$, one finds $\xi \approx 1.98 \pm 0.35$, in agreement with $\xi = d_w/2 = 1.90$, where d_w is the dimension of a random walk on on the incipient percolating cluster in three dimensions.[12]

With the onset of superlocalization, the electronic states are localized at distances much less than the localization length which would result from the microscopic disorder in the bulk material. Thus, even if the Coulomb interaction is screened in the bulk material, the screening will be ineffective when the electronic states become superlocalized. We conclude, therefore, that superlocalization near the percolation threshold will lead to universal transport behavior with the variable-range hopping among superlocalized states always dominated by the Coulomb interaction and with $\gamma = \xi/(\xi + 1) \approx {}^2/_3$.

Acknowledgment. This work was partially supported by the MRL Program of the National Science Foundation under Award No. DMR-9123048 and partially supported by a research grant from the Electric Power Research Institute (EPRI). C.O.Y. was supported by the Korean Science and Engineering Foundation (KOSEF). The PANI–CSA materials were supplied by UNIAX Corp.

References and Notes

(1) (a) Fizazi, A.; Moulton, J.; Rughooputh, S. D. D.; Smith, P.; Heeger, A. J. *Phys. Rev. Lett.* **1990**, *64*, 2180. (b) Suzuki, Y.; Heeger, A. J.; Pincus, P. *Macromolecules* **1990**, *23*, 4730.

(2) Andreatta, A.; Heeger, A. J.; Smith, P. *Polym. Commun.* **1990**, *31*, 275.

(3) Hotta, S.; Rughooputh, S. D. D. V.; Heeger, A. J. *Synth. Met.* **1987**, *22*, 79.

(4) (a) Aldissi, M.; Bishop, A. R. *Polymer* **1985**, *26*, 622. (b) Aldissi, M. *Synth. Met.* **1986**, *13*, 87.

(5) Wang, Y.; Rubner, M. F. *Macromolecules* **1992**, *25*, 3284.

(6) Cao, Y.; Smith, P.; Heeger, A. J. *Synth. Met.* **1992**, *48*, 91.

(7) Reghu, M.; Cao, Y.; Moses, D.; Heeger, A. J. *Phys. Rev. B* **1993**, *47*, 1758.

(8) Yang, C. Y.; Cao, Y.; Smith, P.; Heeger, A. J. *Synth. Met.* **1993**, *53*, 293.

(9) Stauffer, D. *Introduction to Percolation Theory*; Taylor & Francis: Philadelphia, 1985.

(10) Michels, M. A.; Brokken-Zijp, J. C. M.; Groenewoud, W. M.; Knoester, A. *Physica (Amsterdam)* **1989**, *157A*, 529.

(11) Salome, L.; Carmona, F. *Carbon* **1991**, *29*, 599.

(12) Levy, Y. E.; Souillard, B. *Europhys. Lett.* **1987**, *4*, 233.

(13) Mott, N. F.; David, E. *Electronic Properties in Non-Crystalline Materials*; Clarendon: Oxford, 1979.

(14) Deutscher, G.; Levy, Y. E.; Souillard, B. *Europhys. Lett.* **1987**, *4*, 577.

(15) van der Putten, D.; Moonen, J. T.; Brom, H. B.; Brokken-Zijp, J. C. M.; Michels, M. A. J. *Phys. Rev. Lett.* **1992**, *69*, 494.

(16) Alexander, S.; Orbach, R. *J. Phys. (Paris), Lett.* **1982**, *43*, 625.

(17) Aharony, A.; Harris, A. B.; Entin-Wohlman, O. *Phys. Rev. Lett.* **1993**, *70*, 4160.

(18) Michels, M. A. J.; Brokken-Zijp, J. C. M.; van der Putten, D.; Moonen, J. T.; Brom, H. B. *Phys. Rev. Lett.* **1993**, *70*, 4161.

(19) Efros, A. L.; Shklovskii, B. I. *J. Phys. C* **1975**, *8*, 49.